Off-equilibrium dynamics of a (1 + 1)-dimensional directed polymer in random media



1996 J. Phys. A: Math. Gen. 29 1421

(http://iopscience.iop.org/0305-4470/29/7/014)

J. Phys. A: Math. Gen. **29** (1996) 1421–1434. Printed in the UK

# Off-equilibrium dynamics of a (1 + 1)-dimensional directed polymer in random media

Hajime Yoshino

Institute of Physics, University of Tsukuba, Tsukuba, Japan

Received 9 October 1995

**Abstract.** The relaxational dynamics of a $(1 + 1)$-dimensional directed polymer in random potential is studied by Monte Carlo simulations. A series of temperature quench experiments is performed changing waiting times $t_w$. A clear crossover from quasi-equilibrium behaviour ($t \ll t_w$) to off-equilibrium behaviour ($t \gg t_w$) appears in the dynamical overlap function whose scaling properties are very similar to those found in the three-dimensional spin-glass model. In the $t \gg t_w$ part, the fluctuation dissipation theorem of the first kind which relates the response function to the tilt field with the conjugate correlation function, is found violated. These ageing effects are brought about by the very slow growth of the quasi-equilibrium domain driven by successive *loop excitations* of various sizes, which form complex network structures.

## 1. Introduction

Directed polymer in random media (DPRM) [1] is one of the simplest statistical mechanical models in which quenched randomness plays non-trivial roles as in spin-glasses. It is an effective model of an elastic string in a random environment, such as a vortex line in an oxide cuprate superconductor which penetrates the stacked $CuO_2$ layers with point defects scattered randomly over the layers. In transverse dimensions $d$ less than two, there is no *free phase* but a *pinned phase*, i.e. the polymer is mostly pinned around the ground state and cannot move freely at any finite temperatures. However, there are anomalously large thermal fluctuations due to the thermal hoppings between the excited states which are nearly degenerate with the ground state but located far away. They are analogous to the droplet excitations in the spin-glass phase [2] and bring about non-trivial effects in the pinned phase [3–6]. One naturally expects that they also have dramatic effects on the dynamics. Actually, it has been argued in the theory of the transport problem in the vortex glass phase that they are responsible for the nonlinear current–voltage response [7].

Our interest in the present study is the slow relaxation to equilibrium due to such anomalous thermal hoppings. We expect that they bring about ageing effects, which are to some extent similar to those found in the spin-glass phase. In order to clarify this possibility, we performed temperature quench experiments by a simple heat-bath Monte Carlo dynamics. The procedure mimics the so-called IRM experiments in spin-glasses [8] but the system is perturbed by a small *tilt* field which drives one end of the polymer instead of the magnetic field in spin-glasses which drives the whole spins.

We have found clear evidences of the ageing effects. One is the systematic waiting time dependence of the dynamical overlap function. The crossover behaviour from quasi-equilibrium to off-equilibrium behaviour and its scaling properties are, interestingly enough,

0305-4470/96/071421+14$19.50  

very similar to those found in the spin-autocorrelation function of the three-dimensional spin-glass model [10]. The second is the violation of the fluctuation dissipation theorem (FDT) associated with the response to the tilt field. Again the correlation function, which is conjugate with the response function, shows a clear waiting time dependence. On the other hand, in contrast with the case of spin-glasses, the response function itself does not show waiting time dependence. The FDT which relates the two is violated at $t \gg t_w$, which coincides with the crossover behaviour in the dynamical overlap function.

In our analysis we also utilize the transfer matrix method for the following two purposes. Firstly, we check the consistency between the static limit of the data of the dynamical quantities and the static expectation values. Secondly, we study the relation between the complex free energy landscape and the relaxational dynamics. Actually we could visually monitor the thermal jumps between the excited states. The structure of the web of the excited states is very complex and consists of numerous loop-like structures of various sizes (see figure 3 below). Since this model is somewhat simpler than spin-glass models, we believe that understanding the dynamics of this model would give valuable insight into the glassy dynamics of more complicated systems.

This paper is organized as follows. In section 2 we describe our model and introduce the Monte Carlo dynamics. In section 3, the elementary process of the dynamics is studied combined with analysis of the free energy landscape by the transfer matrix method. In section 4, the procedure of the temperature quench experiment is described. The results are given in section 5. In section 6, we conclude this paper with some phenomenological arguments.

## 2. The model

We study a lattice version of a $(1 + 1)$-dimensional directed polymer in random media (DPRM). The Hamiltonian is

$$\mathcal{H}_\mu[x] = \sum_{z=1}^{N} \{g|x(z) - x(z+1)| + \mu(x(z), z)\} - hx(N) \tag{1}$$

where $x(z)$ $(z = 1 \ldots N)$ represents the configuration of the polymer whose length is $N$. As shown in figure 1, the polymer is situated on a square lattice and *directed* along the $z$-axis so that overhangs are excluded. We impose the so-called restricted solid on solid (RSOS) condition, i.e. the steps $|x(z) - x(z-1)|$ are only allowed to take integer values $-1, 0$ and 1. We fix one end $x(0)$ at $x = 0$ while we allow the other end $x(N)$ to move freely. The first term in the Hamiltonian represents the elastic energy. The second term represents the random potential which takes random numbers distributed uniformly over $-\sigma \leqslant \mu \leqslant \sigma$ independently on every lattice site on the square lattice. The last term is the tilt field which drives the free end and *tilts* the polymer.

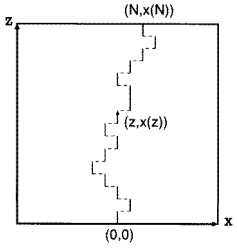


**Figure 1.** A representation of a configuration of $(1 + 1)$-dimensional RSOS DPRM.

We model the relaxational dynamics of the present model by an ordinary heat-bath Monte Carlo dynamics as follows. In one micro Monte Carlo step (micro-MCS), we try to move one segment, say the segment at $z = z_0$. The new position is chosen among the possible choices allowed by the RSOS condition with the appropriate transition probabilities so as to satisfy the detailed balance condition. As shown in figure 2, this micro-MCS can be classified into three cases depending on the positions of the neighbouring segments at $z_0 - 1$ and $z_0 + 1$, namely cases (*a*), (*b*) and (*c*) which corresponds to $|x(z_0 - 1) - x(z_0 + 1)| = 0, 1$ and 2 respectively. The entire configuration is refreshed by vectorized sub-lattice flippings in one Monte Carlo step (MCS) (= $N$ micro-MCS). One sub-lattice consists of the even numbered segments $z = 2, 4, 6 \ldots$ and the other sub-lattice consists of the odd numbered segments $z = 1, 3, 5 \ldots$.

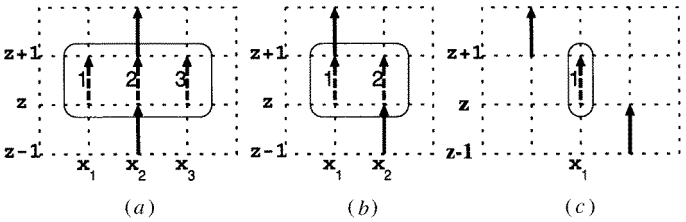


**Figure 2.** The three different cases (*a*), (*b*) and (*c*) of the local configuration around a segment $x(z)$ (see the text for a definition). The possible new states 1, 2 and 3 of the segment $x(z)$ are enclosed by boxes.

## 3. Elementary processes of the dynamics

In this section we consider the elementary processes of the relaxational dynamics in the present model. In any quenched random system, it is generally essential to understand the structure of the free energy landscape in order to study the slow relaxational dynamics, which is unfortunately very hard to do on spin-glass models. However, thanks to the simplicity of the model, we can try such an attempt on the present model in the following way. We consider the spatial variation of $P_\mu(z, x)$: the probability to find the polymer going through a particular lattice point $(z, x)$ on a certain sample of random potential $\mu$. It is defined as

$$P_\mu(z, x) = Z_\mu(z)^{-1} \sum_{\text{configuration}} \delta(x(z) - x)\delta(x(0) - 0) \exp(-\beta \mathcal{H}[x, \mu]) \quad (2)$$

where the sum is taken over all the possible configurations (or paths) $\{x(1), \ldots, x(N)\}$ and $Z_\mu(z)$ is the normalization factor defined so that $\sum_{x=-z}^{z} P_\mu(z, x) = 1$. It is straightforward to calculate this probability by the transfer matrix method [1]. In figure 3, an example of the spatial variation of $P_\mu(z, x)$ of a system of $N = 100$, $T = 0.3$, $g = 0.01$ and $\sigma = 0.5$ on a certain sample of random potential $\mu$ is displayed by a density plot; the intensity increases as the colour becomes brighter. We recognize that most of the probability density is confined in the white *tubes* which are understood as the thermally active excited states. In the dynamics, they presumably serve as *traps* [13], which tend to trap the polymer for long times. On the other hand there are black *voids* between the tubes which presumably serve as free energy barriers. It is quite remarkable that the tubes form a very complicated network which consists of various sizes of loop-like structures. It is qualitatively consistent with the prediction by Hwa and Fisher [4] who have predicted a broad distribution of the

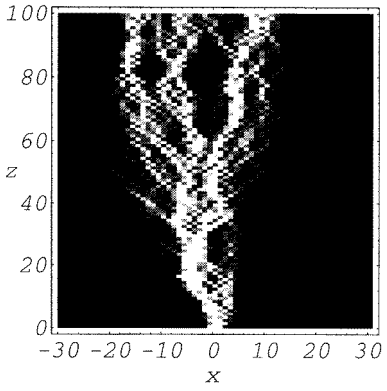


**Figure 3.** The density plot of $P_\mu(z, x)$ (see text for definition) on a certain sample of random potential $\mu$ ($N = 100$, $T = 0.3$, $g = 0.01$ and $\sigma = 0.5$).

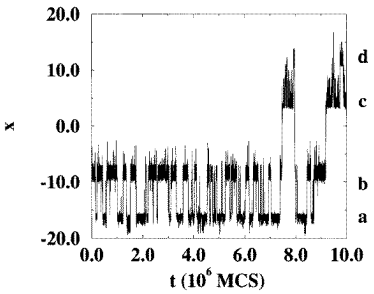


**Figure 4.** A time sequence of $x(80)$ on the same system shown in figure 3. The positions of the four *traps* a, b, c and d are indicated.

size of the loops. As the temperature increases, one can observe that the diameter of the tubes grows and the structure itself changes on large scales as predicted in [3].

From the above observation, we speculate that the dynamics of the polymer roughly consists of two kinds of elementary processes. One is the fast fluctuation within the tubes (traps). The other is the thermally activated jump between such tubes, which is analogous to the droplet excitations in spin-glasses. Actually, these two different processes can be visually monitored rather easily as the following. In figure 4 we plot the time sequence of the segment $x(80)$ on the same systems shown in figure 3. The data are averaged over every interval of $10^3$ (MCS) trying to mask small scale fluctuations. Apart from the remanent small scale fluctuations, which are understood as the fast fluctuations within each trap (tube), the coarse-grained process is apparently understood as jumps between the four traps which correspond to the four major peaks of $P(80, x)$ (white tubes in figure 3 at $z = 80$).

The thermal jumps between the traps must go over the free energy barriers which lie between them (black voids in figure 3). The scaling property of the relaxation times of the thermal jumps between the tubes has already been studied in the context of the aforementioned transport problem in the vortex glass phase [7]. For the convenience of later discussions, we summarize it here. For example, suppose that there is a loop-like structure of tubes as schematically shown in figure 5. Let us denote its transverse size as $\Delta$. Then the free energy barrier $F_{\rm B}(\Delta)$ associated with the thermal excitation over the loop, which we hereafter call *loop excitation* following [7], is expected to scale *typically* as

$$F_{\rm B}(\Delta) \simeq a(T)\Delta^{\alpha} \tag{3}$$

where $a(T)$ is some temperature-dependent constant. The value of the exponent $\alpha$ is expected to be $\frac{1}{2}$ in $1+1$ DPRM [4]. Note that near the free end of the polymer, the tubes do not form complete loop structures but rather *U*-shaped structures in which one side of the

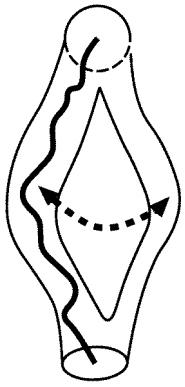

**Figure 5.** A schematic picture of a loop excitation. The polymer (bold curve) inside the left tube jumps over the void to the right tube and vice versa.

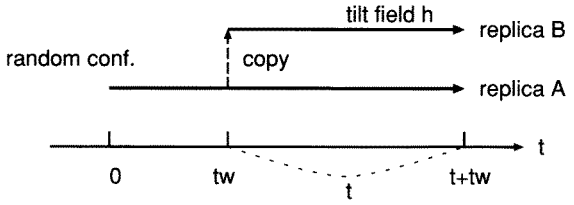


**Figure 6.** The procedure of the temperature quench experiment.

ends of the tubes is left open. But we expect that the free energy barriers of such thermal excitations scale in the same way as the *complete* loop excitations. The relaxation time of the loop excitation is expected to scale *typically* as

$$\tau(\Delta) \sim \exp(F_{\mathrm{B}}(\Delta)/T) \simeq \exp\left(\frac{a(T)\Delta^{\alpha}}{T}\right). \tag{4}$$

The broad distribution of the size of the loops [4] implies broad distribution of relaxation times.

## 4. Procedure of the temperature quench experiment

The numerical experiment is done in the following way (see also the illustration in figure 6). At first, a random initial configuration is prepared. Then the system is allowed to evolve for $t_{\mathrm{w}}$ (MCS) by the heat-bath Monte Carlo dynamics of a certain temperature $T$. This means that the polymer is forced to approach the equilibrium state of temperature $T$ being attached to a heat bath of temperature $T$. After this $t_{\mathrm{w}}$ (MCS) of *ageing*, the polymer's configuration is stored and copied to a replica system. Then we let the two systems, say replicas A and B, continue the relaxational dynamics using the same random numbers (same thermal noise of the heat bath) but applying a small tilt field $h$ to system B.

We measure the following dynamical overlap function as a probe to the relaxational dynamics of the unperturbed system (replica A). It is defined as

$$q(t_{\mathrm{w}}+t, t_{\mathrm{w}}) \equiv \overline{\left\langle \frac{1}{N}\sum_{z=1}^{N} \delta(x^{(\mathrm{A})}(z, t_{\mathrm{w}}+t), x^{(\mathrm{A})}(z, t_{\mathrm{w}}))\right\rangle} \tag{5}$$

where $\delta(x, y)$ is the Kroneker delta and $x^{(\mathrm{A})}(z, t)$ ($z = 1 \ldots N$) represents the configurations of the polymer at $t$ (MCS). Here the bracket $\langle \cdots \rangle$ denotes the average over statistically independent ageing processes and the overbar $\overline{\cdots}$ the average over different realizations

of random potentials. The above overlap function is defined in analogy with the spin-autocorrelation function of the spin-glass models and conveniently measures the 'closeness' between the configurations at two different times $t_w + t$ and $t_w$. In the static limit, it is expected to converge to the expectation value of the overlap $q_{rep}$ between two real replica systems which has been introduced by Parisi [5] and studied numerically by Mézard [6],

$$q_{rep} = q_{static} \equiv \lim_{t\to\infty} \lim_{t_w\to\infty} q(t_w + t, t_w). \tag{6}$$

We measure the dynamical response to the tilt field at $t$ (MCS) after $t_w$ (MCS) of ageing as the distance between the temporal positions of the free end $x(N)$ of the two replicas A and B, which we denote as $x_e^{(A)}(t_w + t)$ and $x_e^{(B)}(t_w + t)$,

$$\overline{\delta x_e(t; t_w)} \equiv \overline{\left\langle x_e^{(B)}(t_w + t) - x_e^{(A)}(t_w + t)\right\rangle}. \tag{7}$$

Note that $\langle\cdots\rangle$ encloses both $x_e^{(A)}(t)$ and $x_e^{(B)}(t)$ because we use the same random numbers in replicas A and B in our procedure. This definition is slightly different from the conventional one $\overline{\left\langle x_e^{(B)}(t_w + t)\right\rangle} - \overline{\left\langle x_e^{(A)}(t_w + t)\right\rangle}$. However our present choice is more efficient in practice because it provides essentially the same result but with less noise.

In equilibrium, the response function (7) is related to the correlation function

$$C_e(t_1, t_2) = \overline{\left\langle x_e^{(A)}(t_1) x_e^{(A)}(t_2)\right\rangle} \tag{8}$$

as

$$\overline{\delta x_e(t; t_w)} = h \int_{t_w}^{t_w+t} R_e(t + t_w, t')\,dt' = \beta h\,[C_e(t_w + t, t_w + t) - C_e(t_w + t, t_w)] \tag{9}$$

by the fluctuation dissipation theorem (FDT) of the first kind,

$$R_e(t_1, t_2) \equiv \overline{\delta x_e(t_1 - t_2; t_2)}/\delta h(t_2) = \beta \partial C_e(t_1, t_2)/\partial t_2 \tag{10}$$

provided that $h$ is small enough (linear response regime). Note that in the static limit $t_w \to \infty$ and $t \to \infty$ of (9), we get the ordinary static FDT,

$$\overline{\langle x_e\rangle_h} = \lim_{t\to\infty} \lim_{t_w\to\infty} \overline{\delta x_e(t_w; t)} = \beta h \chi \tag{11}$$

where the susceptibility $\chi$ is given by

$$\chi = \overline{\left\langle x_e^2\right\rangle - \langle x_e\rangle^2}. \tag{12}$$

We performed a series of temperature quench experiments on the system with various sizes $N = 20, \ldots, 300$, and temperatures at $T = 0.1, \ldots, 0.5$. The parameters $g$ and $\sigma$ are fixed at $g = 0.01$ and $\sigma = 0.5$. The average over $10^4, \ldots, 10^2$ samples of random potential were done depending on the system size. In order to ensure that $h$ is small enough so that the linear response condition is satisfied, we calculated the disorder averaged static susceptibility $\chi$ (see (12)) and $\overline{\langle x_e\rangle_h}$ by the transfer matrix method [6] and checked that (11) is well satisfied.

## 5. Results

### *5.1. Crossover behaviour of the dynamical overlap function*

We first present the results of the dynamical overlap function defined in (5) on the unperturbed system (replica A). The following analysis is done on the data of $N = 300$ at $0.1 < T < 0.5$. The observation was done in the time window ($0 < t < 10^4$ (MCS)) for

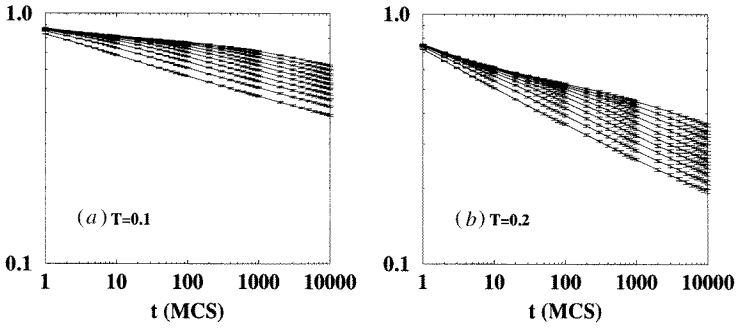


**Figure 7.** The waiting time $t_w$ dependence of $q(t_w, t_w + t)$: $N = 300$, $10^2$ samples at ($a$) $T = 0.1$ and ($b$) $T = 0.2$. The waiting time increases as $t_w = 2, 4, 8, \ldots 1024$ (MCS) from the bottom to the top curve.

$t_w = 2, 2^2, \ldots, 2^{10}$ (MCS). The data at $T = 0.1$ and 0.3 are plotted by a double logarithmic plot in figure 7. The remarkable feature is that the data curves show strong waiting time $t_w$ dependence and each of them drops off rapidly at around $t \sim t_w$. It is presumably understood as a manifestation of the crossover from the quasi-equilibrium behaviour ($t \ll t_w$) to the off-equilibrium behaviour ($t \gg t_w$), i.e. ageing effect. Actually we see later that it coincides with the FDT violation which also occurs at around $t \sim t_w$.

The quasi-equilibrium regime ($t \ll t_w$) begins with an initial fast decay and crosses over to a much slower decay, which is only visible on the data curves of sufficiently large $t_w$. Unfortunately we cannot determine the asymptotic functional form ($t_w \gg 1$) of the latter slow decay at this moment. However, the scaling analysis which we discuss later suggests an algebraic law (see equation (17) below) with very small exponent $x(T)$ which varies with the temperature as shown in figure 10. On the other hand, the off-equilibrium part is fitted well by an algebraic law

$$q(t_w, t_w + t) \sim t^{-\lambda(T)} \qquad (t \gg t_w) \tag{13}$$

where the exponent $\lambda(T)$ also depends on temperature as shown in figure 10. It is interesting to note that these characteristics of the crossover behaviour are very similar to those originally found by Rieger [10] in the spin-autocorrelation function of the three-dimensional Edwards–Anderson spin-glass model in the spin-glass phase.

We now analyse the scaling properties of the dynamical overlap function. We try the scaling form

$$q(t_w, t_w + t) \simeq C(t_w, T)\tilde{q}_T(t/t_w)\,. \tag{14}$$

As an example, the scaling plot of the data of $N = 300$, $T = 0.17$ is shown in figure 8. The parameter $C(t_w, T)$ was chosen so as to scale the off-equilibrium part ($t/t_w \gg 1$) as well as possible. It turns out that the initial fast decay part, which we mentioned before, does not fit on the master curve of the $t/t_w$ scaling. In practice, we could obtain the scaling plot shown in figure 8 discarding the data of $t \leqslant 10$ (MCS). At higher temperatures we have to discard more data to obtain good master curves.

As expected, the scaling function behaves as $\tilde{q}_T(y) \sim y^{-\lambda(T)}$ at $y \gg 1$ with $\lambda(T)$ which we found in (13). On the other hand the constant $C(t_w, T)$ turns out to be well fitted by an algebraic law of $t_w$,

$$C(t_w, T) \sim t_w^{-x(T)} \tag{15}$$

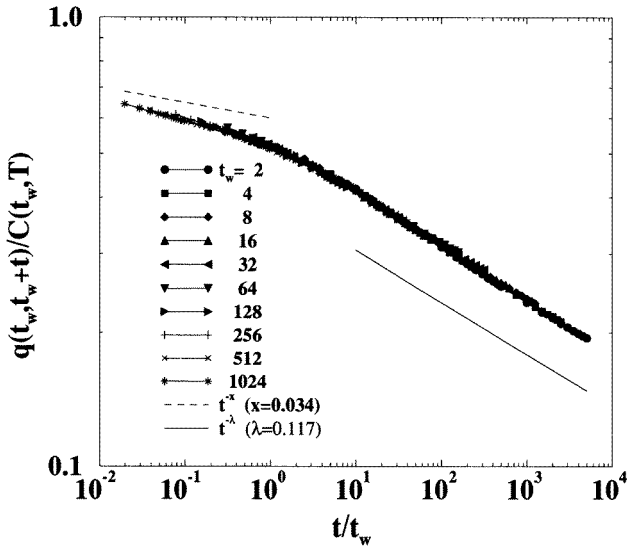


**Figure 8.** A scaling plot of the dynamical overlap function on the system of $N = 300$ and $T = 0.17$ by the scheme (14). The scale of the vertical axis is arbitrary. The broken line represents the power law $t^{-x}$ using $x$ obtained by the fit (15). The full line represents the power law $t^{-\lambda}$ with $\lambda$ obtained by the direct fit of the $t/t_w \gg 1$ part.

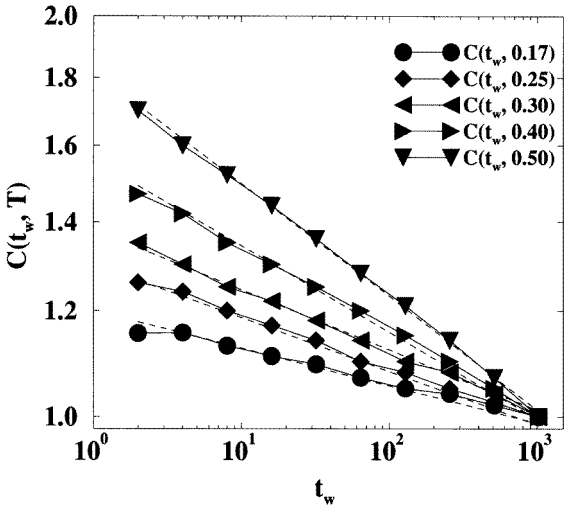


**Figure 9.** Double logarithmic plot of $C(t_w, T)$ versus $t_w$ at $T = 0.17$, 0.25, 0.30, 0.40 and 0.50. The scale of the vertical axis is arbitrary. The broken lines are the fit by the algebraic law (15) with $x(T)$ presented in figure 10.

as shown in figure 9. The exponent $-x(T)$ obtained by this fitting varies with temperature as presented in figure 10. At $T < 0.17$, $-x(T)$ becomes too small to be determined precisely.

Using (15), we can rewrite (14) as

$$q(t_w, t_w + t) \simeq t^{-x(T)} \phi_T(t/t_w) \tag{16}$$

where $\phi_T(y)$ is related to $\tilde{q}_T(y)$ in (14) by $\phi_T(y) \equiv y^{x(T)} \tilde{q}_T(y)$. Note that this scaling form is also identical to that originally found in the three-dimensional spin-glass model by Rieger [10]. The new scaling form (16) implies that the quasi-equilibrium part ($t/t_w \ll 1$) behaves as

$$q(t_w, t + t_w) \sim t^{-x(T)} \qquad (t_w \gg 1 \text{ and } t/t_w \ll 1)\,. \tag{17}$$

However, as can be seen in the master curve in figure 8, the crossover takes place rather gradually and the left branch of the master curve ($t/t_w \ll 1$) seems to decay faster than the expected algebraic law $t^{-x(T)}$ with $x(T)$ obtained from (15). This discrepancy implies that

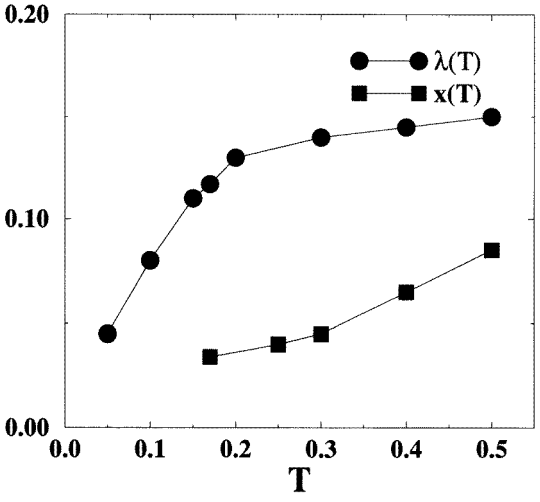


**Figure 10.** Temperature dependence of the exponents: $\lambda(T)$ and $x(T)$. They are obtained from data of ($N = 300$, $10^2$ samples).

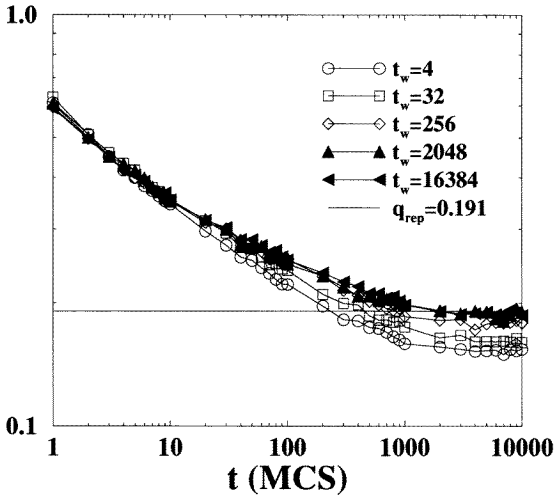


**Figure 11.** Saturation of ageing effect due to the finite size effect ($N = 20$, $T = 0.5$, 500 samples). $q_{\rm rep}$ was calculated by the transfer matrix method.

we have not yet attained the asymptotic scaling region ($t_{\rm w} \gg 1$) of the quasi-equilibrium part ($t/t_{\rm w} \ll 1$). Unfortunately we could not accomplish it with our available computational power.

Lastly we discuss the finite size effects. As far as the system size $N$ is finite, the size of the largest loop excitation and thus the associated maximum relaxation time $\tau_{\rm max}(N)$ available in the system must be finite (see (4)). Thus we expect that system is fully equilibrated if we take $t_{\rm w}$ larger than a certain equilibration time $t_{\rm eq}(N)$ which may be comparable with the $\tau_{\rm max}(N)$. The finite size effect appears in the dynamical overlap function as follows. In figure 11 the data on the system of $N = 20$ and $T = 0.5$ are shown as a typical example. It can be seen that the waiting time $t_{\rm w}$ dependence on the dynamical overlap function saturates at some finite $t_{\rm w}$ as $t_{\rm w}$ is increased: the curves do not show any further $t_{\rm w}$ dependence when $t_{\rm w}$ exceeds some characteristic time $t_{\rm eq}(N)$. In the example shown in figure 11, it is larger than 2048 but less than 16 384 (MCS). We have checked that $t_{\rm eq}(N)$ increases as we increase the system size $N$. It is also recognized that the dynamical overlap function saturates to the static limit $q_{\rm static}$ (see (6)) when $t \gg t_{\rm eq}$. The value of

$q_{\mathrm{static}}$ is nearly equal to $q_{\mathrm{rep}}$ obtained by the transfer matrix method which uses two real replicas [6]. Though $q_{\mathrm{rep}}$ is non-zero in finite systems, further calculations by the transfer matrix method on larger systems show that $q_{\mathrm{rep}}$ decreases as the system size $N$ increases and vanishes in the thermodynamic limit $N \to \infty$ (see [6]).

### *5.2. Violation of FDT*

We next present the results of the response to the tilt field defined in (7). The curves in figure 12 show the LHS and RHS of the FDT relation (9) at different waiting times $t_{\mathrm{w}} = 40$, 200 and 1000 (MCS) on the system of $N = 20$ at $T = 0.2$ with the tilt field $h = 0.1$ by a semi-logarithmic plot. The quench experiment was done over $10^4$ different samples of random potentials in order to take a sufficient average over the disorder. The curves of the LHS of (9) (correlation) strongly depend on the waiting time $t_{\mathrm{w}}$. On the other hand, the curves of the RHS of (9) (response) do not seem to have significant $t_{\mathrm{w}}$ dependence and almost seem to merge with each other within the numerical accuracy. Comparing with the data of larger system sizes, we checked that the data are not spoiled by finite size effects

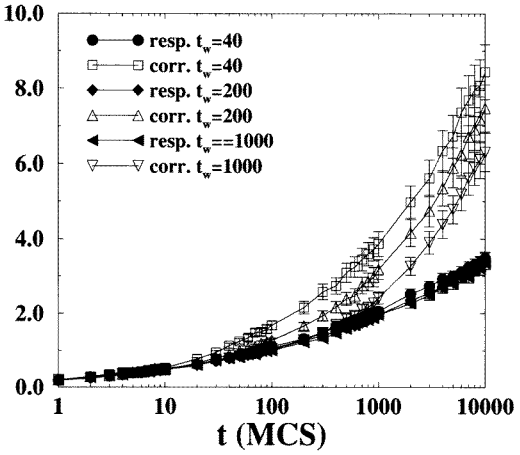


**Figure 12.** FDT relation ($N = 20$, $T = 0.2$, $10^4$ samples). The top three curves are the LHS of (9) (correlation) of different waiting times $t_{\mathrm{w}} = 40$, 200 and 1000 (MCS). The three curves below are the RHS of (9) (response) of the corresponding $t_{\mathrm{w}}$.

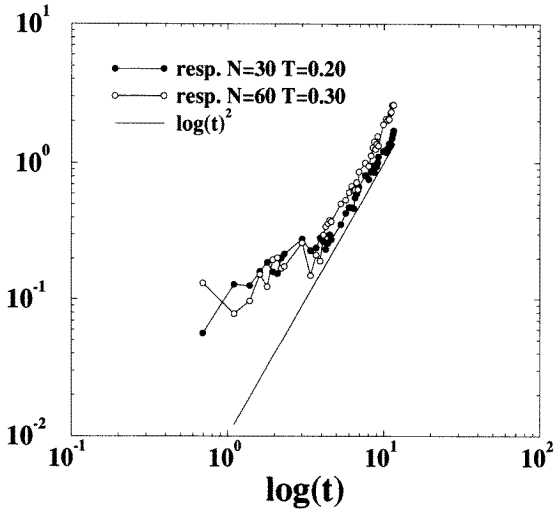


**Figure 13.** Functional form of the response function ($N = 30$, $T = 0.20$, $10^4$ samples and $N = 60$, $T = 0.40$, $5 \times 10^3$ samples with $h = 0.03$). The full line represents the $\log(t)^2$ law (18).

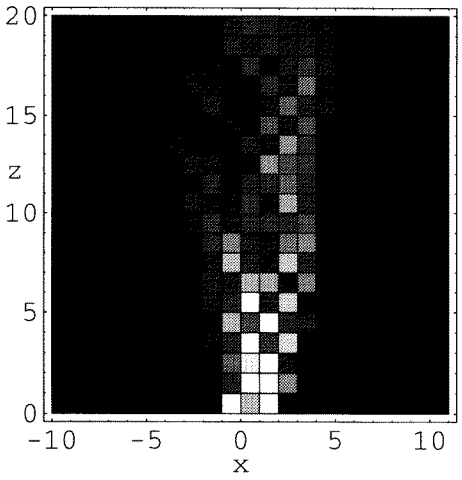


**Figure 14.** The density plot of $P(z, x)$ on a certain sample of a small system at a high temperature ($N = 20$, $T = 1.00$).

within this observation time window ($0 < t < 10^4$ (MCS)). However, it is difficult to get smooth data on larger systems because the sample-to-sample fluctuations between systems of different random potentials are larger on larger systems.

As is clear from the figure, the FDT relation is satisfied in the regime $t \ll t_w$ but broken in the regime $t \gg t_w$. It is again clear evidence of the crossover from quasi-equilibrium to off-equilibrium dynamics, i.e. ageing effect. Similar FDT violation was previously found in the spin-glass phase of the three-dimensional spin-glass models by Monte Carlo simulations [11, 12]. However, there is an important difference: in the spin-glass models both the response and correlation functions strongly depend on $t_w$ while in the present model the response does not seem to have $t_w$ dependence. This is understood as follows. As the tilt field pulls the free end of the polymer, it moves by successive local thermal excitations around it, while the rest of the system is indifferent to the existence of the tilt field. We expect that the free energy barrier of such thermal excitations scales as (3). Thus the response will scale the same way as the *typical* transverse size of a loop excitation which becomes active after waiting time $t$,

$$\overline{\delta x_e(t; t_w)} \sim \log(t)^{1/\alpha}. \tag{18}$$

In order to clarify this scaling form, we performed longer simulations up to $10^5$ (MCS). In figure 13 we show the double logarithmic plot of $\overline{\delta x_e(t; 0)}$ versus $\log(t)$ on the system of $N = 30$, $T = 0.20$ and $N = 60$ at $T = 0.30$ with $h = 0.03$. It can be seen that the behaviour is consistent with (18) with $\alpha = \frac{1}{2}$ and thus supports the above argument. The data on different system sizes and at different temperatures show similar behaviour except that data of smaller systems show saturations within the observation time window.

Lastly we consider the extremely-high-temperature case in finite systems. As we mentioned before, the diameter of the tubes grows as the temperature increases [4]. Then if the system is too small, a single tube swallows up the whole system and the thermal jumps between the tubes disappear. In figure 14 an example is shown of a free energy landscape of such a case, the density plot of $P_\mu(z, x)$ of a system of $N = 20$ at $T = 1.0$ on a certain random potential. Roughly, only a single big tube can be recognized. In such an extreme case, we found no ageing effects. The FDT relation is fulfilled in the whole $t$ range up to the static limit as shown in figure 15. At around $10^3$ (MCS), they saturate to the static limit, $\overline{\langle x_e \rangle_h}$ or $h/T\chi_e$ (see (11)) calculated by the transfer matrix method. In addition, the dynamical overlap function does not show any $t_w$ dependence. These facts suggest that the

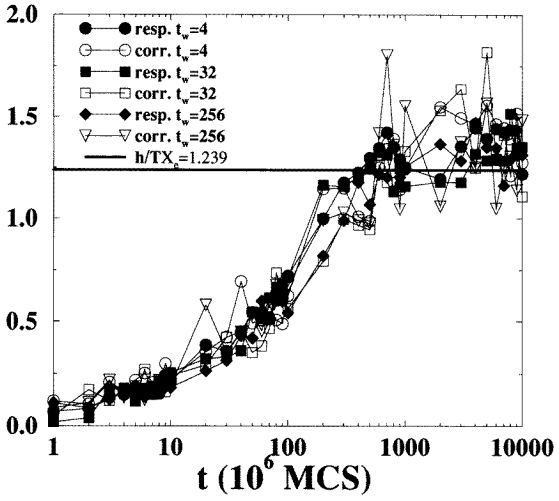


**Figure 15.** The FDT relation (9) of a small system at a high temperature ($N = 20$, $T = 1.00$, $h = 0.1$, 500 samples) for $t_w = 4, 32, 256$ (MCS). The horizontal line is $h/T\chi_e$ where $\chi_e$ (see equation (12)) is obtained by the transfer matrix method.

thermal jumps between the tubes, i.e. loop excitations, are the essential processes to bring about the observed ageing effects.

## 6. Conclusion

The relaxational dynamics of a $(1 + 1)$-dimensional DPRM has been investigated by Monte Carlo simulations which mimic the IRM experiments in spin-glasses. The ageing effect appears as the systematic waiting time dependence on both the dynamical overlap function and the FDT violation. The dynamical overlap function shows a clear crossover from slow quasi-equilibrium decay ($t \ll t_w$) to fast off-equilibrium decay ($t \gg t_w$). The latter is well fitted by an algebraic law whose exponent depends on temperature. The $t/t_w$ scaling scheme works well and it also suggests another algebraic decay in the quasi-equilibrium part. However, we could not confirm the latter directly with our computational power. On the other hand, the response to the tilt field grows as $\log(t)^2$ (18) independently of the waiting times, which supports the assumed scaling properties of loop excitations (see (3) and (4)). Concerning the fact that it does not show $t_w$ dependence, this model appears rather trivial compared with, for example, spin-glasses in which there are also dramatic effects in the response function so that one can actually observe the ageing effects in experiments by measuring the magnetization [7, 8]. None the less, other aspects of the ageing effect are very similar to those found in the spin-glass phase of three-dimensional spin-glass models [9–11]. Hence we believe that this model provides a good testing ground for various theoretical ideas of the slow dynamics of quenched random systems.

The important elementary processes to bring about the observed ageing effect are the loop excitations, i.e. thermal hoppings between the traps (tubes) in the free energy landscape. They have been actually demonstrated by direct monitoring of the time sequences. Thus the equilibration process is understood as the slow growth of a quasi-equilibrium domain driven by successive loop excitations. Note that this growth mechanism of the quasi-equilibrium domain is essentially the same as that proposed in the spin-glass models in which droplet excitations drive the growth of the domain [2]. From (4), we expect that its transverse size $R(t_w)$ grows with the waiting time $t_w$ as

$$R(t_w) \sim \log(t_w)^{1/\alpha}. \tag{19}$$

However, the scaling properties of the dynamical overlap function are not trivial. Although they turned out to be quite similar to those found in the spin-glass model [10], they cannot be explained by simply borrowing the assumptions of the above-mentioned droplet theory of spin-glass [2]. In the droplet theory, it is assumed that

$$q(t, 0) \sim R(t)^{-\lambda} \tag{20}$$

where $q(t_1, t_2)$ is now the spin-autocorrelation function and $\lambda$ is some unknown exponent [2]. (Here $\lambda$ is the notation of [2] and different from $\lambda(T)$ defined in (13).) But we do not have any reason to believe that such a relation exists in the present model, and actually our result (13) cannot be consistent with (19) if we assume (20). In the study of a spin-glass model [10], it is argued that (13) can be consistent with (20) if one assumes that the free energy barrier grows logarithmically with its transverse size $\Delta$ rather than algebraically so that $R(t)$ grows algebraically with a certain temperature-dependent exponent. If it is also the case in the present model, the response function (7) should be fitted by such an algebraic law. However, our data of the response function show systematic curvature in double logarithmic plots and do not prefer such an algebraic law but the logarithmic law (18). Thus we conclude that the simple relation (20) does not exist in the present model. The scaling properties of the dynamical overlap function require other ways to explain them.

The important feature we recognize in figure 3 is that the tubes are grouped together to form some very complicated network. We already know how the relaxation time associated with each single loop excitation scales with its transverse size (see (4)). However, there is an obvious but important rule: a loop excitation can *flip* only when some parts of the temporal configuration of the polymer actually stay either side of the loop, in other words the *empty* loops cannot *flip*. It should also be noted that the polymer is *not* allowed to be broken into pieces during the dynamical process. Thus the entire loop excitations built in the system cannot become *active* simultaneously but only those which are associated with the sequence of the loops which contains the actual temporal configuration of the polymer. From the above considerations, it is clear that the information on the connectivity of the loops is an important ingredient to describe the whole dynamics of the polymer properly.

Let us now consider the dynamical overlap function (5). It can be roughly interpreted as the *probability* that the segments of the polymer return to the original traps in which they initially stay after jumping around other traps in the network. Here we need the detailed description of the dynamics mentioned above since the probability is the sum of the probabilities associated with all of the possible trajectories which make such return trips. Each of these trajectories consists of different sequences of loop excitations which vary in size and thus have different relaxation times. It is unlikely that there is a single *typical* mode whose probability dominates the total probability. On the other hand, the response to the tilt field may not depend directly on such details but just scales as the *expectation value* of the transverse size of the local loop excitation around the free end which can become active after waiting time $t$. It is possible that such an expectation value is dominated by the contribution from the *typical* mode whose relaxation time is comparable with $t$. We think this is the reason why we could obtain (18) using only the scaling property of single loop excitation.

Although the network apparently looks quite complicated, a most simple characterization of it will be the following. The network structure consists of loops of various sizes which are hierarchically nested so that larger ones enclose smaller ones inside. (A similar picture was proposed before by Villain concerning the organization of *droplets* in spin-glass phase, see [14].) From this simple picture, the dynamics can be regarded as one of the hierarchical diffusion processes which have been intensively studied in rather abstract contexts, for

example the *ultradiffusion* models [16]. It is interesting to note that in the latter models the autocorrelation function (return probability) shows asymptotically algebraic decay with some temperature-dependent exponent, which is also the case in the dynamical overlap function in the present model. Furthermore, it has already been shown by Sibani and Hoffmann that hierarchical diffusion processes can show ageing effects [15]. Thus it will be fruitful to construct a phenomenological theory of the ageing effect of the present model from this point of view. A study in this direction will be reported elsewhere [17].

*Note added in proof.* We received a preprint by L F Cugliandolo, J Kurchan and L Drossal who studied the off-equilibrium dynamics of a manifold in random potential using mean-field theory [18]. It would be valuable to compare the results of the mean-field approaches with the simulations of low-dimensional systems in future works.

## Acknowledgments

The author would like to sincerely thank Professor H Takayama for valuable discussions and critical reading of the manuscript. He would also like to thank Dr H Reiger, Professors K Nemoto, K Hukusima and T Komori for stimulating discussions. This work was supported by a Grant-in-Aid for Scientific Research from the Ministry of Education, Science and Culture, Japan. The author was supported by Fellowships of the Japan Society for the Promotion of Science for Japanese Junior Scientists.

## References

[1] For a recent review of DPRM and various related topics, see Halpin-Healy and Zhang Y C 1995 *Phys. Rep.* **254**
[2] Fisher D S and Huse D A 1988 *Phys. Rev.* B **38** 373, 386
[3] Fisher D S and Huse D A 1991 *Phys. Rev.* B **43** 10 728
[4] Hwa T and Fisher D S 1994 *Phys. Rev.* B **49** 3136
[5] Parisi G 1990 *J. Physique* **51** 1595
[6] Mézard M 1990 *J. Physique* **51** 1831
[7] Fisher D S, Fisher M P A and Huse D A 1991 *Phys. Rev.* B **43** 130
[8] Lundgren L, Svedlindh P, Nordblad P and Beckmann O 1983 *Phys. Rev. Lett.* **51** 911
[9] Refregier Ph, Vincent E, Hammann J and Ocio M 1987 *J. Physique* **48** 1553
[10] Rieger H 1993 *J. Phys. A: Math. Gen.* **26** L615
[11] Anderson J O, Mattson J and Svedlindh D 1992 *Phys. Rev.* B **46** 8297
[12] Franz S and Rieger H 1995 *J. Stat. Phys.* **79** 704
[13] Bouchaud J P 1992 *J. Physique* **2** 1705
[14] Villain J 1986 *Europhys. Lett.* **2** 871
[15] Sibani P and Hoffmann K H 1989 *Phys. Rev. Lett.* **63** 2853
[16] Bachas C P and Huberman B A 1987 *J. Phys. A: Math. Gen.* **20** 4995 and references therein
[17] Yoshino H in preparation
[18] Cugliandolo L F, Kurchan J and Drossal L 1995 *Preprint* cond-mat.9509009
see also Cugliandolo L F and Kurchan J 1993 *Phys. Rev. Lett.* **71** 1; 1994 *J. Phys. A: Math. Gen.* **27** 5749